Biochemical and Biophysical Research Communications 454 (2014) 493–499

Contents lists available at ScienceDirect

Biochemical and Biophysical Research Communications

journal homepage: www.elsevier.com/locate/ybbrc

Fluorescent labelling of intestinal epithelial cells reveals independent long-lived intestinal stem cells in a crypt

Nobukatsu Horita [a,1], Kiichiro Tsuchiya [b,*,1], Ryohei Hayashi [a,c], Keita Fukushima [a], Shuji Hibiya [a], Masayoshi Fukuda [a], Yoshihito Kano [a], Tomohiro Mizutani [a], Yasuhiro Nemoto [a], Shiro Yui [a], Ryuichi Okamoto [b], Tetsuya Nakamura [b], Mamoru Watanabe [a]

[a] Department of Gastroenterology and Hepatology, Graduate School, Tokyo Medical and Dental University, Japan
[b] Department of Advanced Therapeutics for Gastrointestinal Diseases, Graduate School, Tokyo Medical and Dental University, Japan
[c] Department of Gastroenterology and Metabolism, Hiroshima University, Japan

ARTICLE INFO

Article history:
Received 7 October 2014
Available online 29 October 2014

Keywords:
Imaging of a single stem cell
Intestinal stem cells
Long-lived stem cells

ABSTRACT

Background and aims: The dynamics of intestinal stem cells are crucial for regulation of intestinal function and maintenance. Although crypt stem cells have been identified in the intestine by genetic marking methods, identification of plural crypt stem cells has not yet been achieved as they are visualised in the same colour.
Methods: Intestinal organoids were transferred into Matrigel® mixed with lentivirus encoding mCherry. The dynamics of mCherry-positive cells was analysed using time-lapse imaging, and the localisation of mCherry-positive cells was analysed using 3D immunofluorescence.
Results: We established an original method for the introduction of a transgene into an organoid generated from mouse small intestine that resulted in continuous fluorescence of the mCherry protein in a portion of organoid cells. Three-dimensional analysis using confocal microscopy showed a single mCherry-positive cell in an organoid crypt that had been cultured for >1 year, which suggested the presence of long-lived mCherry-positive and -negative stem cells in the same crypt. Moreover, a single mCherry-positive stem cell in a crypt gave rise to both crypt base columnar cells and transit amplifying cells. Each mCherry-positive and -negative cell contributed to the generation of organoids.
Conclusions: The use of our original lentiviral transgene system to mark individual organoid crypt stem cells showed that long-lived plural crypt stem cells might independently serve as intestinal epithelial cells, resulting in the formation of a completely functional villus.

1. Introduction

The intestinal environment varies according to the effects of different luminal substances, such as digested food and bacteria [1]. Therefore, to maintain its homeostasis, the intestine needs to adapt to the variable environment. Coordination of the various epithelial cells in each villus is critical for adapting to a variable environment. Intestinal stem cells at the base of crypts maintain individual villi by generating various types of epithelial cells over a lifetime [2]. It has been suggested that various cell signalling pathways [3] and transcription factors [4] destine epithelial cells to a specific cell lineage. However, the fate of intestinal stem cells themselves is not well understood. Previous reports have indicated that groups of stem cells are located in a crypt and act as reservoirs to continuously supply various types of cells to the villi over a lifetime [5]. Different subpopulations of intestinal stem cells, as defined by Lgr5 [6], Bmi1 [7], Lrig1 [8], mTert [9] and HopX [10] expression, have been demonstrated by genetic marking methods, a finding that has led to questions about which populations lie ancestrally upstream of others [11]. However, it has been reported that tamoxifen might ablate stem cells and induce regeneration of intestinal epithelial cells [11]. Further, a functional approach independent of stem cell markers has been reported. Continuous clonal labelling using the relative instability of dinucleotide repeat tracts during

Abbreviations: CBC, crypt base columnar; TA, transit amplifying; GFP, green fluorescence protein gene; Lgr5, leucine-rich-repeat-containing G-protein-coupled receptor 5; OLFM4, Olfactomedin 4.

* Corresponding author at: Department of Advanced Therapeutics for Gastrointestinal Diseases, Graduate School, Tokyo Medical and Dental University, 1-5-45 Yushima, Bunkyo-ku, Tokyo 113-8519, Japan. Fax: +81 3 5803 0268.
E-mail address: kii.gast@tmd.ac.jp (K. Tsuchiya).

[1] The first two authors have contributed equally to this work.

http://dx.doi.org/10.1016/j.bbrc.2014.10.091
0006-291X/

DNA replication has demonstrated both lower stem cell numbers per crypt and lower stem cell replacement rates [12]. These studies suggest that previous inferences of stem cell numbers and replacement rates derived from pulse-chase labelling may be overestimated. Thus, identification and tracking of individual stem cells in crypts would be helpful for understanding the dynamics of the fate of crypt stem cells. Most importantly, the Cre-loxP system is unable to detect individual stem cells in a crypt *in vivo* or *in vitro* because all previous stem cell markers are expressed in the plural cells at the base of a crypt [13].

In vitro organoid culture of intestinal epithelial cells while maintaining the crypt formation enables assessment of the dynamics of epithelial cells visually and sequentially [14,15]. However, it is difficult to directly introduce a transgene into the organoids for visualisation of a particular cell because of the matrix around the organoids. In this study, we applied an original approach independent of stem cell-specific markers to visualise stem cells in an organoid.

2. Materials and methods

2.1. Cell culture and chemicals

Human embryonic kidney-derived 293T cells were cultured in Dulbecco's modified Eagle's medium (Sigma, St. Louis, MO, USA) supplemented with 10% foetal bovine serum and 1% penicillin–streptomycin. Culture of the intestinal epithelium was performed as described previously [16]. Crypts of the proximal small intestine were obtained from adult heterozygous mice harbouring an Lgr5-EGFP-IRES-creERT2 knock-in allele and were purified. They were counted and embedded in Matrigel® (BD Biosciences, San Jose, CA) at 10,000 crypts/ml. For conventional culture, 30 μl of Matrigel® was seeded on 24-well plates. For live imaging experiments, 60 μl of Matrigel® was placed in 35-mm culture dishes. The medium was changed every 2 days. For cell passage, the medium was discarded and the Matrigel® was dissolved by the Cell Recovery Solution® (BD, Franklin Lakes, NJ, USA). The organoids were washed twice with phosphate buffer solution (PBS) and mechanically dissociated into crypt domains level by pipetting. Then transferred into fresh Matrigel® and organoid culture medium as above. The interval of cell passage was approximately once every week, with a 1:3 ratio for amplification. When necessary, Hoechst33342 (04915-81; Nacalai tesque) was added to the medium as indicated. Animal experiments were performed with the approval of the Institutional Animal Care and Use Committee of Tokyo Medical and Dental University.

2.2. Lentivirus infection to the organoids

Lentivirus production was performed according to the manufacturer's protocols. Lenti-virus supernatants were concentrated using Lenti-X™ (Clontech Laboratories, Inc.), leading to 100-folds increase in virus titer. Equal parts of the mixture of Matrigel® and virus solution and 293T cells were mixed together. After the mixture solidified, culture medium was overlaid. For the infection into the organoid, the medium was discarded and the Matrigel® was dissolved by the Cell Recovery Solution® (BD, Franklin Lakes, NJ, USA). The organoids were washed twice with PBS and mechanically dissociated into crypt domains level by pipetting. Then transferred into Matrigel® and mixed with equal parts of the lentivirus solution. The organoids in Matrigel® were divided into two wells in a 24-well plate. Organoid culture medium was overlaid after the Matrigel® solidified. The infection of the organoids was repeated three times during the passage of the organoids.

2.3. 3-Dimentional fluorescence analysis

Hoechst33342 was added to the medium for 10 min to detect the nuclei of organoids. After discarding the medium, 4% paraformaldehyde was added for 6 h to fix the organoids. Then the organoids in Matrigel® were put on a slide and mounted with VectaShield mounting medium (H-1000; Vector Laboratories, Burlingame, CA, USA). Whole organoids were visualised by confocal laser fluorescent microscopy FLUOVIEW FV10i (Olympus, Tokyo, Japan) to acquire high-resolution images of the specimens (optical section, 5 μm; *Z*-axis increment, 1 μm). Fluorescence from mCherry and Hoechst33342 was detected using filter sets for mCherry (excitation, 559 nm; emission, 610 nm) and Hoechst33342 (excitation, 405 nm; emission, 455 nm), respectively. A 3 dimensional (3D) picture was constructed from the sequential imaging of a whole organoid using FV10-ASW 3.1 software (Olympus).

2.4. Time-lapse live cell imaging

Live imaging was performed on the Delta Vision system (Applied Precision, Washington, USA) incorporating a fluorescent microscope IX-71 (Olympus) using a 20× 0.75NA UPlanSApo objective (Olympus). Fluorescence from mCherry was detected using filter sets for mCherry (excitation, 577/25; emission, 632/60). Time-lapse experiments were performed as previously described [16]. Differential interference contrast (DIC) and fluorescent images were acquired at 15-min intervals for 30 h or 45 h. The data were processed using softWoRx® (Applied Precision, Issaquah, WA) and, if necessary, image editing was performed using Adobe Photoshop CS5.1. Maximum intensity projections of the time series were exported into QuickTime format for presentation as Supplementary Movies.

3. Results

3.1. Lentivirus mixed into Matrigel enables direct infection of organoids

We first assessed the efficacy of the transgenic system that uses a lentivirus for gene transfer into an organoid. 293T cells were placed in a dish with or without Matrigel®, and lentiviruses coding for the green fluorescence protein (GFP) gene were added to the medium. The 293T cells in Matrigel® did not show green fluorescence, whereas 293T cells seeded on the dish showed fluorescence, which suggested that the lentiviruses were unable to pass through the Matrigel® (Fig. 1A). The lentiviruses were therefore mixed into the Matrigel® with 293T cells, which resulted in production of green fluorescence from the 293T cells in the Matrigel® (Fig. 1B). We used this method to introduce the mCherry fluorescence gene as a transgene into organoids generated from mouse small intestines. Although one-time introduction of the transgene did not lead to mCherry fluorescence even though mCherry gene expression was detected in the organoids (Supplementary Fig. 1), threefold repeated introduction of the transgene did lead to detection of mCherry fluorescence in the organoids (Fig. 1C). We isolated a single organoid with mCherry fluorescence by observation under a stereoscopic microscope (Fig. 1D); this single organoid was then mechanically divided into several pieces by using a needle to expand the organoids (Supplementary Fig. 2). After expansion, the divided organoids were removed from the Matrigel® and mechanically dissociated into the crypts by using a plastic pipette tip for continuous passage (Fig. 1E). Culture of these organoids for >1 year showed continuous mCherry fluorescence in every crypt of all organoids, which suggested that the mCherry gene had been transgenically introduced into the stem cells. Further analysis using confocal microscopy showed heterogeneous distribution of

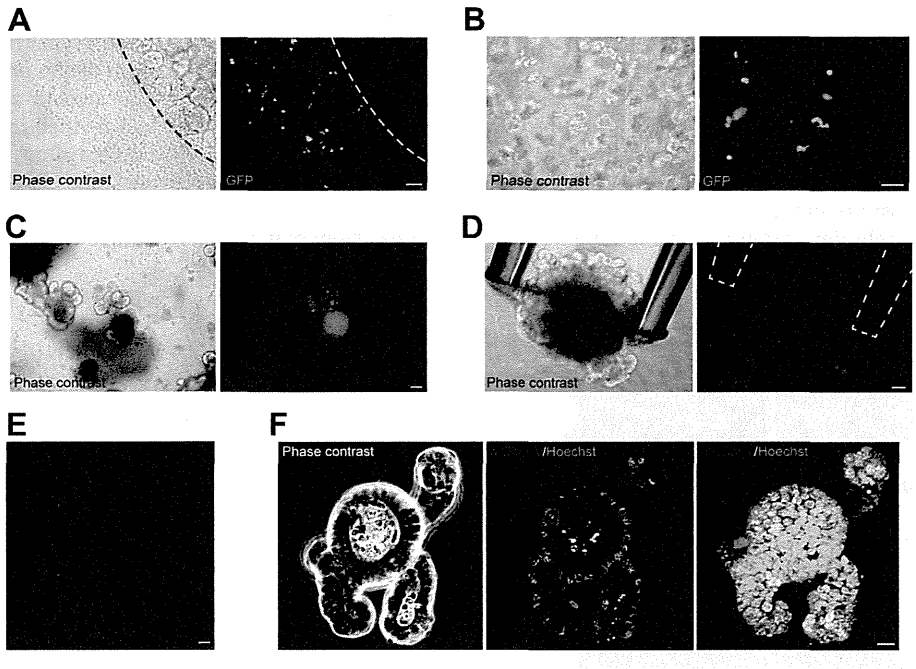

Fig. 1. Gene transduction into organoids resulted in the continuous fluorescence. (A) Lentiviruses coding for the green fluorescence protein gene were added to the medium. 293T cells mounted into the Matrigel® were not fluorescent (right side of each picture) whereas the 293T cells at the dish bottom were fluorescent (left side of each picture). (B) 293T cells mounted into the Matrigel® mixed with lentiviruses were fluorescent. (C) The organoids generated from small intestines were mounted into the Matrigel® mixed with lentivirus encoding the mCherry gene. The organoids were fluorescent after three times lentivirus infections. (D) A single organoid with mCherry fluorescence was collected into a plastic pipette tip. Scale bar: 50 μm. (E) mCherry fluorescent organoids expanded from a single organoids. Scale bar: 200 μm. (F) Heterogeneous expression of mCherry fluorescence in an organoid (mCherry-hetero organoid) over a year after the infection with lentiviruses. Left and centre panels are confocal imaging of an infected organoid. Right panel is 3-dimensional imaging of a whole organoid constructed by confocal microscopy. Scale bar: 10 μm.

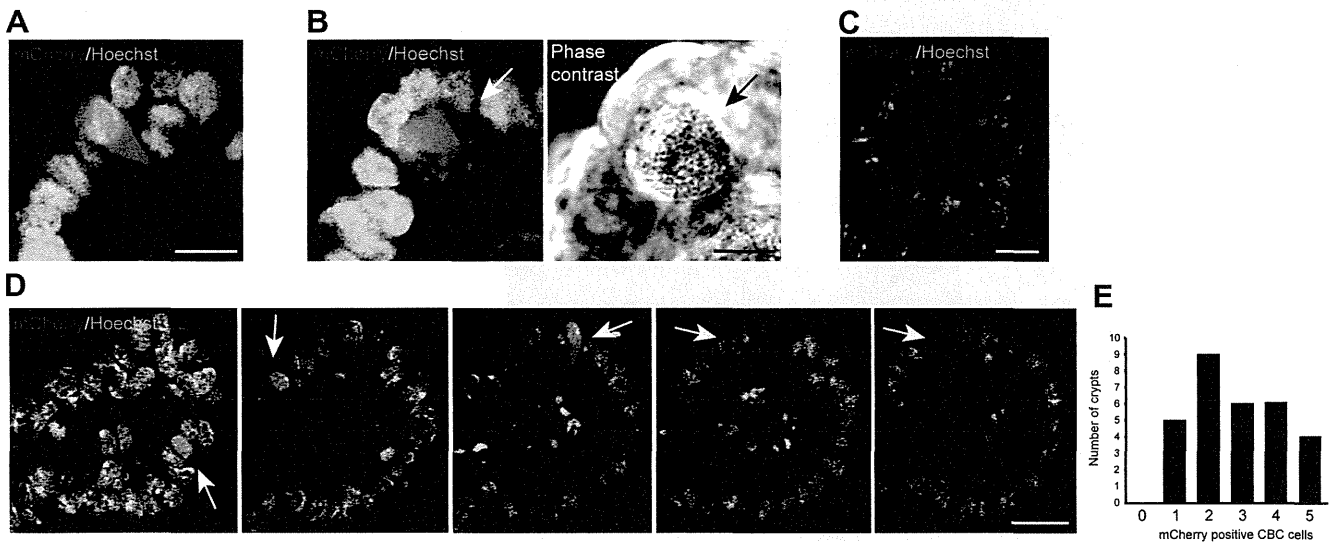

Fig. 2. Partial infection of the organoids enables the marking of individual stem cells in a crypt. (A) An mCherry positive crypt base columnar (CBC) cell in a crypt with a spindle shape. Green fluorescence protein fluorescence marking Lgr5 expression is lost after long-time culture. (B) An mCherry positive Paneth cell in a crypt with broad shape and granules. Scale bar: 5 μm. (C) Confocal imaging of a single mCherry-positive CBC cell in a crypt. 3D imaging of whole crypt is shown in Supplementary Movie 1. Scale bar: 10 μm. (D) Confocal imaging of five mCherry-positive CBC cells in a crypt. Sequential imaging of a whole crypt is shown in Supplementary Movie 2. Scale bar: 15 μm. (E) The number of mCherry-positive CBC cells in each 30 crypts of the mCherry-hetero organoids was counted. The maximum number of mCherry-positive CBC cells in a crypt was 5. No mCherry negative crypts were shown in all organoids.

the mCherry-positive cells in every crypt of all organoids (mCherry-hetero organoids) (Fig. 1F) (Supplementary Table 1).

3.2. Partial infection into the organoids allows the marking of individual stem cells

Because we could morphologically distinguish crypt base columnar (CBC) cell as a spindle shape cell from Paneth cell as a granular cell in the crypt (Fig. 2A and B), we counted the number of mCherry-positive CBC cells in the crypts that resulted in 1–5 mCherry-positive cells in each crypt (Fig. 2C–E, Supplementary Movies 1 and 2).

3.3. Fluorescent labelling of intestinal epithelial cells shows the different stem cells in a crypt

Our findings suggested that a single stem cell might be unable to occupy all intestinal cells in a crypt and villi. Staining of the

small intestinal stem cell specific marker, Olfactomedin 4 (OLFM4) [17] showed that OLFM4 was expressed in both mCherry-positive and -negative cells in the same crypt of mCherry-hetero organoids that have been cultured for >1 year (Fig. 3A). Moreover, HopX as a quiescent +4 stem cell marker and Musashi-1 as a CBC stem cell marker were also expressed in both mCherry-positive and -negative cells in the same crypt of mCherry-hetero organoids, suggesting that mCherry-positive and -negative cells might include stem cells (Fig. 3A). Paneth cells detected by lysozyme staining of a whole organoid were also derived from both mCherry-positive and -negative stem cells in the same crypt (Fig. 3B, Supplementary Movie 3). Time-lapse observation of the organoids in which only an mCherry-positive cell was located in a crypt revealed that a single mCherry-positive cell had divided into two cells. Finally, a single mCherry-positive cell supplied almost all CBC cells in a crypt in addition to transit amplifying (TA) cells (Fig. 3C, Supplementary Movies 4 and 5). However, the heterogeneity of mCherry expression has been maintained during continuous passages for >1 year,

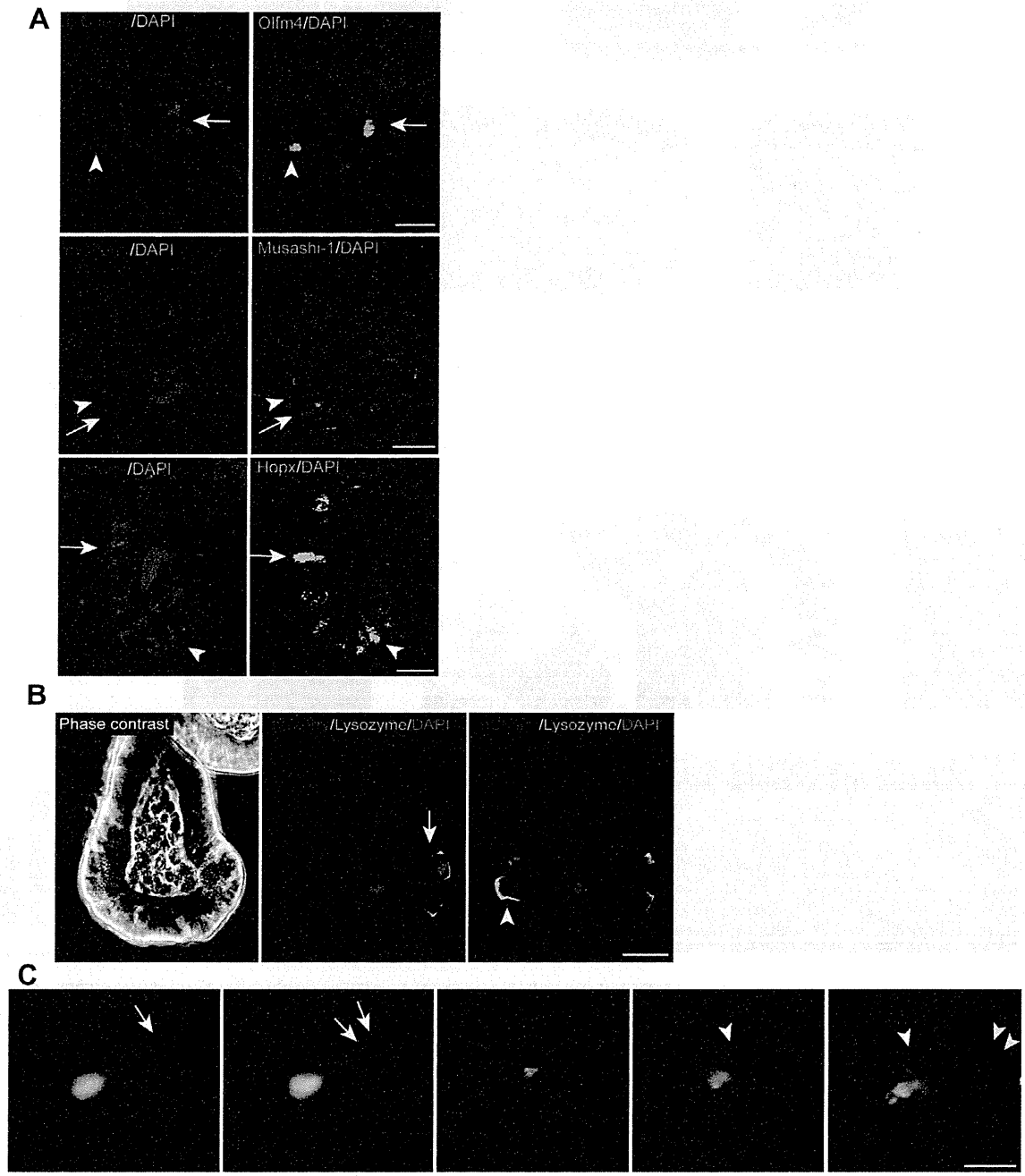

Fig. 3. Heterogeneity of intestinal stem cells in a crypt is maintained for over 1 year. (A) Immunofluorescent staining of mCherry and OLFM4, Musashi-1 and HopX (green) in serial sections of the mCherry-hetero organoid. OLFM4, Musashi-1 and HopX were expressed in both mCherry-positive (arrow) and -negative cells (arrow head) in the same crypt. Scale bar: 20 μm. (B) Immunofluorescent staining of mCherry and Lysozyme (green) in a whole mCherry-hetero organoid. Sequential confocal imaging shows both mCherry-positive (arrow) and -negative (arrow head) cells in a crypt. 3D imaging of a whole crypt is shown in Supplementary Movie 3. Scale bar: 20 μm. (C) Time lapse imaging of an organoid that has a single mCherry-positive cell in a crypt. 16 h 44 min later, a single mCherry-positive cell was divided into two cells (arrow). Following the first cell division, mCherry-positive cells supplied cells to the transit amplifying zone (white arrowhead) and crypt base (yellow arrowhead) for 45 h. Time lapse movies are shown in Supplementary Movie 4, 5. Scale bar: 50 μm. (For interpretation of the references to colour in this figure legend, the reader is referred to the web version of this article.)

which suggests that plural stem cells might fundamentally exist in a crypt to alternatively produce intestinal epithelial cells for the villi and crypt base.

3.4. Individual stem cells in a crypt can enable the generation of organoids

To characterise the mCherry-positive and -negative cells, we dissociated the mCherry-hetero organoids into individual cells (Fig. 4A). The organoids developed from a single cell showed that mCherry-positive and -negative organoids were individually generated (Fig. 4B). Each organoid was isolated under a stereoscopic microscope. Observation using confocal microscopy of whole organoids revealed that all cells expressed mCherry in the mCherry-positive organoids and that no cells expressed mCherry in the mCherry-negative organoids (Fig. 4C, Supplementary Movies 6–9). These findings indicate that both mCherry-positive and -negative cells in a crypt of the mCherry-hetero organoids have the capacity to generate organoids. Moreover, mCherry-negative organoids generated from mCherry-hetero organoids never became fluorescent again for >1 year, supporting the independency of mCherry-positive/negative stem cells in mCherry-hetero organoids. The

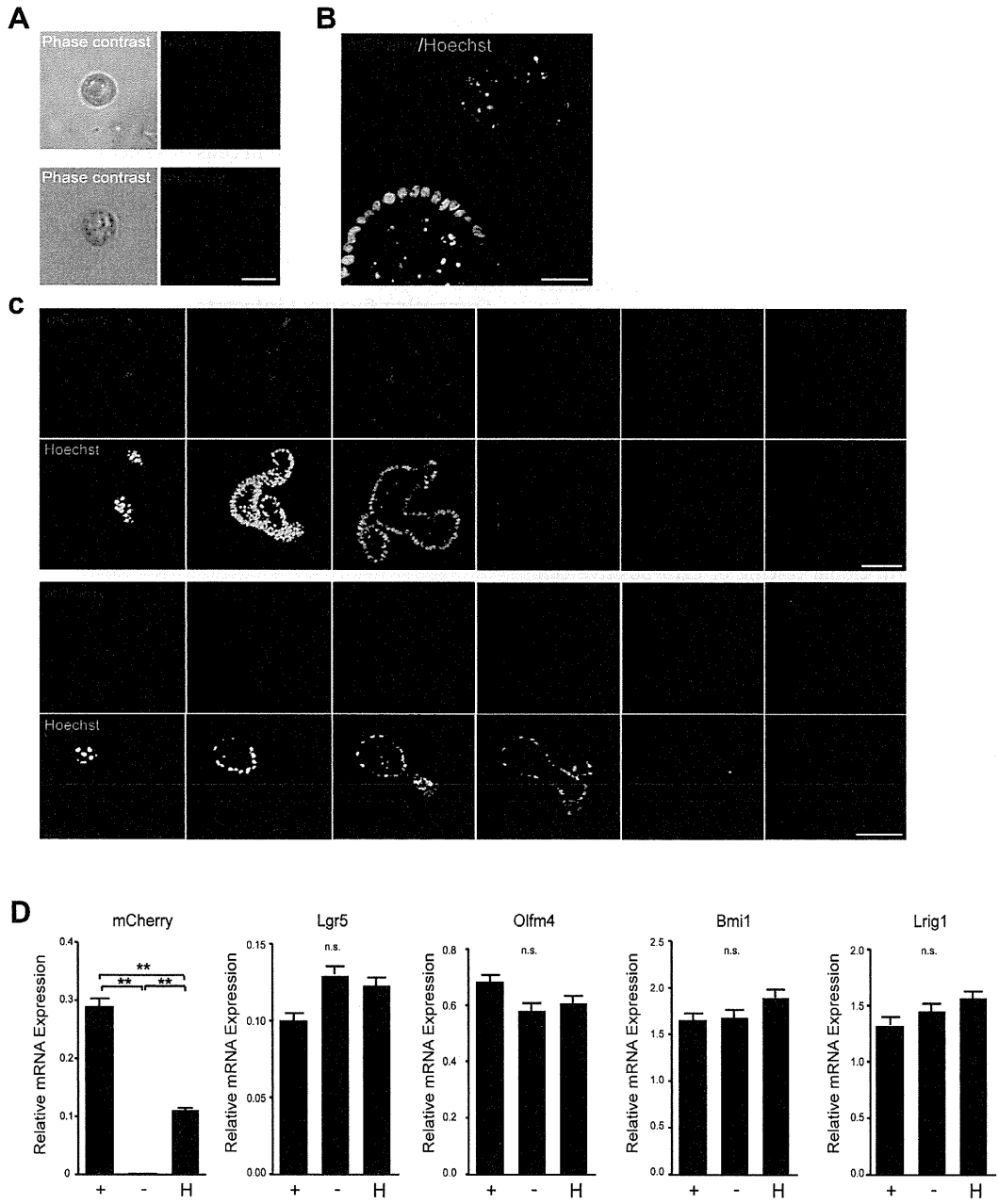

Fig. 4. Both mCherry-positive and -negative single cell reconstruct organoids. (A) mCherry-hetero organoids were dissociated as a single-cell level. Individual mCherry-positive and -negative cells were together mounted into the Matrigel® and cultured. Scale bar: 5 μm. (B) The organoids generated from a single mCherry-positive and -negative cell 7 days after the single-cell dissociation. Scale bar: 20 μm. (C) Sequential confocal imaging of a whole organoid. All cells were mCherry positive in an organoid generated from a single mCherry-positive cell (upper panel) whereas all cells were mCherry negative in an organoid generated from a single mCherry-negative cell (lower panel). Sequential imaging of a whole organoid is also shown in Supplementary Movies 6–9. Scale bar: 50 μm. (D) Quantitative real-time polymerase chain reaction (RT-PCR) for mCherry expression. +, completely mCherry-positive organoids generated from a single mCherry-positive cell in mCherry-hetero organoids. –, completely mCherry-negative organoids generated from a single mCherry-negative cell in mCherry-hetero organoids. H, mCherry-hetero organoid cultured for >1 year. Quantitative RT-PCR for intestinal stem cell markers. No significant differences were observed among the three organoids.

expression of the mCherry gene was greater in mCherry-positive organoids than in mCherry-hetero organoids, whereas mCherry-negative organoids did not express the mCherry gene (Fig. 4D). Finally, each organoid was characterised to confirm whether long-lived plural stem cells in the same crypt shared the functions of a villi and a crypt, resulting in the equal expression of a series of stem cell markers in each organoid (Fig. 4D).

4. Discussion

This study showed that plural stem cells in a crypt may be long-lived and produce different types of intestinal epithelial cells in villi. Although the use of lentivirus mixed with Matrigel® led to partial introduction of the transgene into organoids, random marking of the organoid cells showed that regulation of specific cell types, including stem cells, had occurred. Previous reports have indicated that individual cells dissociated from organoids could be inoculated with a transgene by retroviruses without Matrigel® [18]. Our method however enabled the introduction of a transgene into organoids in which the original morphology of the stem cells in a crypt *in vivo* might be kept. In particular, we could for the first time, visualise individual stem cells in a crypt which reflected the original position of stem cells *in vivo*. Sequential passages of the organoids generated from a single mCherry-hetero organoid for >1 year indicates that individual mCherry-positive cells in a crypt might be a long-lived stem cell.

Moreover, for the first time, we could divide the long-lived stem cells in a crypt into two subpopulations according to mCherry fluorescence. Previous reports have indicated that Cre-mediated recombination of stem cell marker promoters was useful for detection of intestinal stem cells [6]. However, all stem cells were marked at the same time, which made it impossible to distinguish each stem cell in a crypt. Recently, it has been reported that stem cells could be divided into four subpopulations according to colouring in a confetti mouse model [19]. Long-term clonal tracing of Lgr5-positive cell subpopulations in the confetti mouse resulted in the unification to a single colour in the villi, which suggested that a few long-lived stem cells in a crypt might serve all intestinal epithelial cells in the villi. However, it remains unknown whether individual stem cells in a crypt could supply all cells in a crypt and a villus. In this study, we found that a single mCherry-positive cell was located in a crypt, which suggested that mCherry-negative stem cells might supply almost all intestinal epithelial cells in a crypt and TA zone. Once an mCherry-positive stem cell shifts to the active phase, it supplies almost all CBC cells and TA cells. At the next passage of the organoids, the population of mCherry-positive cells in the crypt was reset, which suggests that individual long-lived stem cells alternately supply almost all CBC cells and TA cells. The observation of 1–5 mCherry-positive CBC cells in each mCherry-hetero organoid might have been caused by the difference in the time phase of mCherry-positive cell division.

Accordingly, these findings raised a question about whether individual long-lived stem cells in a crypt divide into the same cells. The organoids generated from individual long-lived stem cells distinguished by mCherry fluorescence showed no difference about the expression of stem cell markers, which suggests that these two subpopulations of stem cells have the equal capacity of stemness.

In the future, the comparison of gene expression between mCherry-positive and -negative cells in an organoid might be helpful to understand the difference among the subpopulations of the stem cells in a crypt. Although the general cell lineages of the intestine are regulated by a series of transcriptional factors [20], it remains unknown how the ratio of the respective cell lineages are regulated in each villus. In particular, the gene expression profiling is longitudinally different throughout the entire small intestine without Notch signal influence [21], although the differentiation-determined transcriptional factor Atoh1 was directly repressed by Hes1 via Notch signal [22]. This finding suggested that the comportment of stem cells with permanent lineage directivity in a crypt might be changed to adjust the proper cell distribution. In the future, an *in vivo* single-cell tracking method should be used to assess the lineage directivity of each intestinal stem cell in a crypt. Moreover, it remains unknown as to how many long-lived stem cells exist in a crypt because single colour markings of cells divided into only two subpopulations. Multi-colour markings of individual cells in a crypt might clarify the number of long-lived stem cells.

Another valuable feature of this system is that the dynamics of single stem cell in a crypt can be assessed. We could select the crypts in which single stem cell was marked by mCherry. Time-lapse analysis can be used to chronologically assess the regulation of a long-lived stem cell, such as cell quiescence, division, occupation of CBC cells and supply to differentiated cells. Time-lapse analysis would also be useful for determining the effects of various reagents on a stem cell to develop treatments that target intestinal stem cells. A system capable of measurement of single stem cell function should be established in the future.

In conclusion, the use of our novel lentivirus transgene system to mark individual stem cells in a crypt of an organoid demonstrated plural long-lived stem cells in a crypt.

Competing financial interests

The authors declare no competing financial interests.

Author contributions

K.T., M.W., T.N., R.O., Y.K., S.Y., T.M. and Y.N. conceived of and designed the experiments. N.H., R.H, K.F, and M.F. performed the experiments. S.H., K.T. and N.H. analysed the data. N.H. and K.T. wrote the manuscript.

Writing assistance

Crimson Interactive Pvt. Ltd.

Acknowledgments

This study was supported in part by grants-in-aid for Scientific Research, 21590803, 21790651, 21790653, 23130506, 25130704 and 25114703 from the Japanese Ministry of Education, Culture, Sports, Science and Technology; Intractable Diseases, the Health and Labor Sciences Research Grants from the Japanese Ministry of Health, Labor and Welfare; Research Center Network for Realization of Regenerative Medicine from Japan Science and Technology Agency (JST).

Appendix A. Supplementary data

Supplementary data associated with this article can be found, in the online version, at http://dx.doi.org/10.1016/j.bbrc.2014.10.091.

References

[1] R. Eri, M. Chieppa, Messages from the inside. The dynamic environment that favors intestinal homeostasis, Front. Immunol. 4 (2013) 323.
[2] H. Cheng, C. Leblond, Origin, differentiation and renewal of the four main epithelial cell types in the mouse small intestine. V. Unitarian theory of the origin of the four epithelial cell types, Am. J. Anat. 141 (1974) 537–561.
[3] T. Nakamura, K. Tsuchiya, M. Watanabe, Crosstalk between Wnt and Notch signaling in intestinal epithelial cell fate decision, J. Gastroenterol. 42 (2007) 705–710.
[4] Q. Yang, N. Bermingham, M. Finegold, H. Zoghbi, Requirement of Math1 for secretory cell lineage commitment in the mouse intestine, Science 294 (2001) 2155–2158.

[5] C.S. Potten, C. Booth, D.M. Pritchard, The intestinal epithelial stem cell: the mucosal governor, Int. J. Exp. Pathol. 78 (1997) 219–243.
[6] N. Barker, J.H. van Es, J. Kuipers, P. Kujala, M. van den Born, M. Cozijnsen, A. Haegebarth, J. Korving, H. Begthel, P.J. Peters, H. Clevers, Identification of stem cells in small intestine and colon by marker gene Lgr5, Nature 449 (2007) 1003-U1001.
[7] E. Sangiorgi, M.R. Capecchi, Bmi1 is expressed in vivo in intestinal stem cells, Nat. Genet. 40 (2008) 915–920.
[8] A.E. Powell, Y. Wang, Y. Li, E.J. Poulin, A.L. Means, M.K. Washington, J.N. Higginbotham, A. Juchheim, N. Prasad, S.E. Levy, Y. Guo, Y. Shyr, B.J. Aronow, K.M. Haigis, J.L. Franklin, R.J. Coffey, The pan-ErbB negative regulator Lrig1 is an intestinal stem cell marker that functions as a tumor suppressor, Cell 149 (2012) 146–158.
[9] R.K. Montgomery, D.L. Carlone, C.A. Richmond, L. Farilla, M.E. Kranendonk, D.E. Henderson, N.Y. Baffour-Awuah, D.M. Ambruzs, L.K. Fogli, S. Algra, D.T. Breault, Mouse telomerase reverse transcriptase (mTert) expression marks slowly cycling intestinal stem cells, Proc. Natl. Acad. Sci. USA 108 (2011) 179–184.
[10] N. Takeda, R. Jain, M.R. LeBoeuf, Q. Wang, M.M. Lu, J.A. Epstein, Interconversion between intestinal stem cell populations in distinct niches, Science 334 (2011) 1420–1424.
[11] Y. Zhu, Y.F. Huang, C. Kek, D.V. Bulavin, Apoptosis differently affects lineage tracing of Lgr5 and Bmi1 intestinal stem cell populations, Cell Stem Cell 12 (2013) 298–303.
[12] S. Kozar, E. Morrissey, A.M. Nicholson, M. van der Heijden, H.I. Zecchini, R. Kemp, S. Tavaré, L. Vermeulen, D.J. Winton, Continuous clonal labeling reveals small numbers of functional stem cells in intestinal crypts and adenomas, Cell Stem Cell 13 (2013) 626–633.
[13] J. Muñoz, D.E. Stange, A.G. Schepers, M. van de Wetering, B.K. Koo, S. Itzkovitz, R. Volckmann, K.S. Kung, J. Koster, S. Radulescu, K. Myant, R. Versteeg, O.J. Sansom, J.H. van Es, N. Barker, A. van Oudenaarden, S. Mohammed, A.J. Heck, H. Clevers, The Lgr5 intestinal stem cell signature: robust expression of proposed quiescent '+4' cell markers, EMBO J. 31 (2012) 3079–3091.
[14] T. Sato, R.G. Vries, H.J. Snippert, M. van de Wetering, N. Barker, D.E. Stange, J.H. van Es, A. Abo, P. Kujala, P.J. Peters, H. Clevers, Single Lgr5 stem cells build crypt-villus structures in vitro without a mesenchymal niche, Nature 459 (2009) 262–265.
[15] S. Yui, T. Nakamura, T. Sato, Y. Nemoto, T. Mizutani, X. Zheng, S. Ichinose, T. Nagaishi, R. Okamoto, K. Tsuchiya, H. Clevers, M. Watanabe, Functional engraftment of colon epithelium expanded in vitro from a single adult Lgr5$^+$ stem cell, Nat. Med. 18 (2012) 618–623.
[16] T. Mizutani, T. Nakamura, R. Morikawa, M. Fukuda, W. Mochizuki, Y. Yamauchi, K. Nozaki, S. Yui, Y. Nemoto, T. Nagaishi, R. Okamoto, K. Tsuchiya, M. Watanabe, Real-time analysis of P-glycoprotein-mediated drug transport across primary intestinal epithelium three-dimensionally cultured in vitro, Biochem. Biophys. Res. Commun. 419 (2012) 238–243.
[17] J. Schuijers, L.G. van der Flier, J. van Es, H. Clevers, Robust Cre-mediated recombination in small intestinal stem cells utilizing the olfm4 locus, Stem Cell Rep. 3 (2014) 234–241.
[18] B.K. Koo, D.E. Stange, T. Sato, W. Karthaus, H.F. Farin, M. Huch, J.H. van Es, H. Clevers, Controlled gene expression in primary Lgr5 organoid cultures, Nat. Methods 9 (2012) 81–83.
[19] H.J. Snippert, L.G. van der Flier, T. Sato, J.H. van Es, M. van den Born, C. Kroon-Veenboer, N. Barker, A.M. Klein, J. van Rheenen, B.D. Simons, H. Clevers, Intestinal crypt homeostasis results from neutral competition between symmetrically dividing Lgr5 stem cells, Cell 143 (2010) 134–144.
[20] R. Okamoto, K. Tsuchiya, Y. Nemoto, J. Akiyama, T. Nakamura, T. Kanai, M. Watanabe, Requirement of Notch activation during regeneration of the intestinal epithelia, Am. J. Physiol. Gastrointest. Liver Physiol. 296 (2009) G23–G35.
[21] M. Iwasaki, K. Tsuchiya, R. Okamoto, X. Zheng, Y. Kano, E. Okamoto, E. Okada, A. Araki, S. Suzuki, N. Sakamoto, K. Kitagaki, T. Akashi, Y. Eishi, T. Nakamura, M. Watanabe, Longitudinal cell formation in the entire human small intestine is correlated with the localization of Hath1 and Klf4, J. Gastroenterol. 46 (2011) 191–202.
[22] X. Zheng, K. Tsuchiya, R. Okamoto, M. Iwasaki, Y. Kano, N. Sakamoto, T. Nakamura, M. Watanabe, Suppression of hath1 gene expression directly regulated by hes1 via notch signaling is associated with goblet cell depletion in ulcerative colitis, Inflamm. Bowel Dis. 17 (2011) 2251–2260.

PeerJ

Distinct expression patterns of Notch ligands, Dll1 and Dll4, in normal and inflamed mice intestine

Hiromichi Shimizu[1], Ryuichi Okamoto[1,2], Go Ito[1], Satoru Fujii[1], Toru Nakata[1], Kohei Suzuki[1], Tatsuro Murano[1], Tomohiro Mizutani[1], Kiichiro Tsuchiya[1,3], Tetsuya Nakamura[1,3], Katsuto Hozumi[4] and Mamoru Watanabe[1]

[1] Department of Gastroenterology and Hepatology, Tokyo Medical and Dental University, Tokyo, Japan
[2] Center for Stem Cell and Regenerative Medicine, Tokyo Medical and Dental University, Tokyo, Japan
[3] Department of Advanced Therapeutics for GI Diseases, Tokyo Medical and Dental University, Tokyo, Japan
[4] Department of Immunology, Tokai University School of Medicine, Isehara, Japan

ABSTRACT

Reports have suggested that the two Notch ligands, Dll1 and Dll4, are indispensable to maintain the homeostasis of the intestinal epithelium. However, within the intestinal epithelium, the precise distribution of the cells that express those ligands at the protein level remains largely unknown. Here, we show a series of immunohistochemical analysis through which we successfully identified mice intestinal epithelial cells (IECs) that endogenously express Dll1 or Dll4. Results showed that Dll1-positive (Dll1+ve) IECs reside exclusively within the crypt, whereas Dll4-positive (Dll4+ve) IECs can locate both in the crypt and in the villus of the small intestine. Also in the colon, Dll1+ve IECs resided at the lower part of the crypt, whereas Dll4+ve IECs resided at both upper and lower part of the crypt, including the surface epithelium. Both Dll1+ve and Dll4+ve IECs were ATOH1-positive, but Hes1-negative cells, and located adjacent to Hes1-positive cells within the crypts. A sub-population of both Dll1+ve and Dll4+ve IECs appeared to co-express Muc2, but rarely co-expressed other secretory lineage markers. However, as compared to Dll1+ve IECs, Dll4+ve IECs included larger number of Muc2-postive IECs, suggesting that Dll4 is more preferentially expressed by goblet cells. Also, we identified that Dll4 is expressed in the Paneth cells of the small intestine, whereas Dll1 and Dll4 is expressed in the c-kit-positive IECs of the colon, indicating that Dll1+ve and Dll4+ve IECs may contribute to constitute the intestinal stem cell niche. Compared to the normal colon, analysis of DSS-colitis showed that number of Dll1+ve IECs significantly decrease in the elongated crypts of the inflamed colonic mucosa. In sharp contrast, number of Dll4+ve IECs showed a significant increase in those crypts, which was accompanied by the increase in number of Hes1-positive IECs. Those Dll4+ve IECs were mostly found adjacent to the Hes1-positive IECs, suggesting that Dll4 may act as a major Notch ligand in the crypts of the inflamed colonic mucosa. Our results illustrate distinct expression patterns of Dll1 and Dll4 within the intestinal epithelium, and suggest that these two ligands may have different roles in normal and inflamed mucosa.

Submitted 29 January 2014
Accepted 12 April 2014
Published 1 May 2014

Corresponding author
Ryuichi Okamoto,
rokamoto.gast@tmd.ac.jp

Academic editor
Yeong Yeh Lee

Additional Information and Declarations can be found on page 15

DOI 10.7717/peerj.370

How to cite this article Shimizu et al. (2014), Distinct expression patterns of Notch ligands, Dll1 and Dll4, in normal and inflamed mice intestine. *PeerJ 2:e370; DOI 10.7717/peerj.370*

Subjects Histology, Gastroenterology and Hepatology
Keywords Dll1, Dll4, Hes1, ATOH1, Notch signaling, Intestinal epithelial cells, Colitis

INTRODUCTION

The intestinal epithelium is maintained by the rapid renewal of cells that are fueled by the stem cells residing at the lower part of the crypt (*Crosnier, Stamataki & Lewis, 2006*; *Barker, 2013*). Studies have identified that Lgr5-positive crypt base columnar cells definitely function as intestinal stem cells (*Barker et al., 2007*). These cells give rise to ATOH1-positive (ATOH1+ve) secretory-progenitor cells, or Hes1-positive (Hes1+ve) enterocyte-committed progenitor cells, which subsequently differentiate into one of the 5 types of mature cells. During such a process, various molecular signaling pathways including Notch plays distinct roles to maintain stem cell property (*VanDussen et al., 2012*; *Clevers, 2013*), and to organize proper proliferation and differentiation (*Nakamura, Tsuchiya & Watanabe, 2007*; *Vooijs, Liu & Kopan, 2011*).

Notch signaling is a pathway that is mediated by ligand–receptor interaction between neighboring cells (*Artavanis-Tsakonas, Rand & Lake, 1999*). So far, 4 receptors and 5 ligands have been identified in mammalians (*Hori, Sen & Artavanis-Tsakonas, 2013*). In the intestine, it has been shown that several components of the Notch pathway, including the 4 receptors and the 5 ligands are expressed during the developmental period and also during the adulthood (*Schröder & Gossler, 2002*). Studies in mice have shown that Notch1 and Notch2 are indispensable receptors to maintain the homeostasis of the intestinal epithelium (*Riccio et al., 2008*). Also, deletion of both Dll1 and Dll4 resulted in complete silencing of Notch activation within the intestinal epithelium, and thereby induced loss of stem-progenitor population, and a significant increase in number of secretory cells (*Pellegrinet et al., 2011*).

Recent report using Dll1-lacZ reporter mice have shown that Dll1 and Dll4 is expressed by the same population of intestinal epithelial cells (IECs) in the mice small intestine (*Stamataki et al., 2011*). Another report using *in situ* hybridization and a Dll1 knock-in mice showed that Dll1 is expressed in IECs at the +5 position, and those Dll1-positive (Dll1+ve) cells may exist as secretory lineage progenitor cells, and also as a back-up reservoir of stem cells (*van Es et al., 2012*). However, it remains unclear how the IECs that endogenously express the Dll1 protein locate within the crypt-villus unit, and possibly contribute to activate Notch signaling in their neighboring cells (*van Den Brink, de Santa Barbara & Roberts, 2001*). A recent report has shown that expression of Dll1 and Dll4 are directly regulated by the pro-secretory transcription factor, ATOH1, and may function as a key molecule to mediate lateral inhibition between equipotent progenitors (*Kim et al., 2014*). Nevertheless, the precise expression patterns of those ligands in the colon have never been described.

Here, we established an immunohistochemical method through which we can clearly identify cells that express Dll1 or Dll4 at the endogenous level. Results showed that Dll1 and Dll4 are expressed by a distinct subset of ATOH1+ve IECs that locates adjacent to Hes1+ve IECs in the small intestinal and colonic crypts. Moreover, Dll1+ve and Dll4+ve IECs

appeared to change their dominance within the elongated crypts of the colitic mucosa, and thereby contribute to increase the number of Hes1+ve IECs. Thus, the present report clearly illustrates the differential expression patterns of Dll1 and Dll4 along the crypt-villus axis, under normal and colitic environment.

MATERIALS & METHODS

Mice

C57BL/6J mice at 6–8 weeks of age were purchased from Japan Clea (Tokyo, Japan). Lgr5-EGFP- ires- CreERT2 mice (Stock No. 008875) and R26R-lacZ mice (Stock No. 003309) were purchased from The Jackson Laboratory (Bar Harbor, Maine, USA). Dll1-floxed mice (*Hozumi et al., 2004*) and Dll4-floxed mice (*Hozumi et al., 2008*) have been previously described. To generate Lgr5- EGFP- ires- CreERT2/ $Dll1^{fl/fl}$ mice or Lgr5- EGFP- ires- CreERT2/ $Dll4^{fl/fl}$ mice, each floxed mice were crossed with Lgr5- EGFP- ires- CreERT2 mice. Mice carrying the R26R-LacZ allele served as control (Lgr5- EGFP- ires- CreERT2/ R26R-LacZ). Those mice were housed in the animal facility of Tokyo Medical and Dental University. All animal experiments were approved by the Institutional Animal Care and Use Committee of Tokyo Medical and Dental University (Approval Number 0140053A).

Induction of Cre-mediated recombination

Induction of Cre-mediated gene recombination was induced by intraperitoneal injection of Tamoxifen (2 mg/body; SIGMA-ALDRICH, Missouri, USA) dissolved in corn oil for 5 consecutive days. Those mice were sacrificed at the indicated days after the first injection, and subjected to tissue analysis.

Induction of colitis

Induction of colitis was performed as previously described (*Okayasu et al., 1990*; *Okamoto et al., 2009*; *Yui et al., 2012*). Briefly, mice were fed *ad libitum* with 3% Dextran sodium sulfate (DSS, Ensuiko, Yokohama, Japan) for five consecutive days, followed by distilled water for another five days. Mice fed with distilled water alone served as control. Mice were subjected to tissue analysis at the end of the experimental period (Day 10).

Staining analysis of intestinal tissues

Immunostaining of mice intestinal tissues were done as previously described (*Okamoto et al., 2009*; *Yui et al., 2012*). Briefly, intestinal tissues were fixed in 4% parafolmaldehyde, and embedded in OCT compound (Sakura, Tokyo, Japan). 6 μm sections were prepared for staining. Primary antibodies used in the present study are summarized in Table 1. Microwave treatment (500 W, 10 min) in 10 mM citrate buffer was required for staining Dll1, Dll4, Hes1 and ATOH1. Tyramide signal amplification (Molecular Probes, California, USA) was used for immunofluorescent detection of Dll1, Dll4, Hes1 and ATOH1. Staining was visualized by secondary antibodies or Tyramide substrates conjugated with Alexa-594 or Alexa-488 (Molecular Probes, California, USA). Data were collected using a conventional epifluorecent microscope (BZ-8000 or BZ-X700, KEYENCE, Tokyo, Japan)

Table 1 **Primary antibodies used for immunohistochemical staining.**

Antibody	Dilution	Supplier	Product no.	City	Country
Anti-Dll1	1:500	R&D systems	AF5026	Minneapolis	USA
Anti-Dll4	1:500	R&D systems	AF1389	Minneapolis	USA
Anti-Hes1	1:80000	A kind gift from Dr. T Sudo, Toray Industry		Kanagawa	Japan
Anti-ATOH1	1:200	A kind gift from Dr. JE Johnson, UT Southwestern		Dallas	USA
Anti-Ki-67	1:50	DAKO	TEC-3	Glostrup	Denmark
Anti-MUC2	1:100	Santa Cruz Biotechnology	Sc15334	Texas	USA
Anti-ChgA	1:1000	Diasorin	SP-1	Saluggia	Italy
Anti-DLCK1	1:100	Abgent	AP7219B	San Diego	USA
Anti-Lysozyme	1:1500	DAKO	EC3.2.1.17	Glostrup	Denmark
Anti-c-kit	1:100	R&D systems	AF1356	Minneapolis	USA
Anti-GFP	1:500	Nakalai Tesque	GF090R	Kyoto	Japan

or a confocal fluorescent microscope (FLUOVIEW FV10i; OLYMPUS, Tokyo, Japan). LacZ staining of the intestinal tissues were done as previously described (*Barker et al., 2007*).

Quantification of the immunostaining

Number of positive staining cells was quantified by analyzing at least 100 crypts or villi that were randomly selected from 3 individual mice. Two independent investigators, who were not informed of the origin of the tissues or the targets of the staining, collected the data. Those data were statistically analyzed with Welch's *t*-test.

RESULTS

Dll1+ve and Dll4+ve IECs show distinct distribution pattern within the small intestinal and colonic epithelium

As previous studies have suggested that mRNA of Dll1 might be expressed within the mice intestinal epithelium (*Schröder & Gossler, 2002*; *Crosnier et al., 2005*; *Stamataki et al., 2011*; *van Es et al., 2012*), we sought to establish a method to identify cells that endogenously express Dll1 or Dll4 protein at their cell membrane, and thereby function as Notch signal-sending cells. By using a specific antibody for Dll1 or Dll4, we found that a positive staining can be yielded within the intestinal epithelium of the mice small intestine and the colon (Figs. 1A and 1D).

The specificity of those antibodies were validated and affirmed by conditional knockout of Dll1 or Dll4. By using mice carrying either the Dll1-floxed allele or the Dll4-floxed allele in addition to LGR5-EGFP-ires-CreERT2 allele, we induced genetic deletion of either Dll1 or Dll4 in LGR5-EGFP positive intestinal stem cells, and also in their progenies. In those knockout tissues, a clear abolishment of the positive staining in the progenies of EGFP-positive intestinal stem cells was confirmed in a gene-specific manner (Fig. S1).

Positive staining of both Dll1 and Dll4 showed a membranous pattern confirming that the staining demonstrates proteins that are bound to the membrane (Figs. 1B and 1E). However, the distribution of those cells along the crypt-villus axis showed a clear

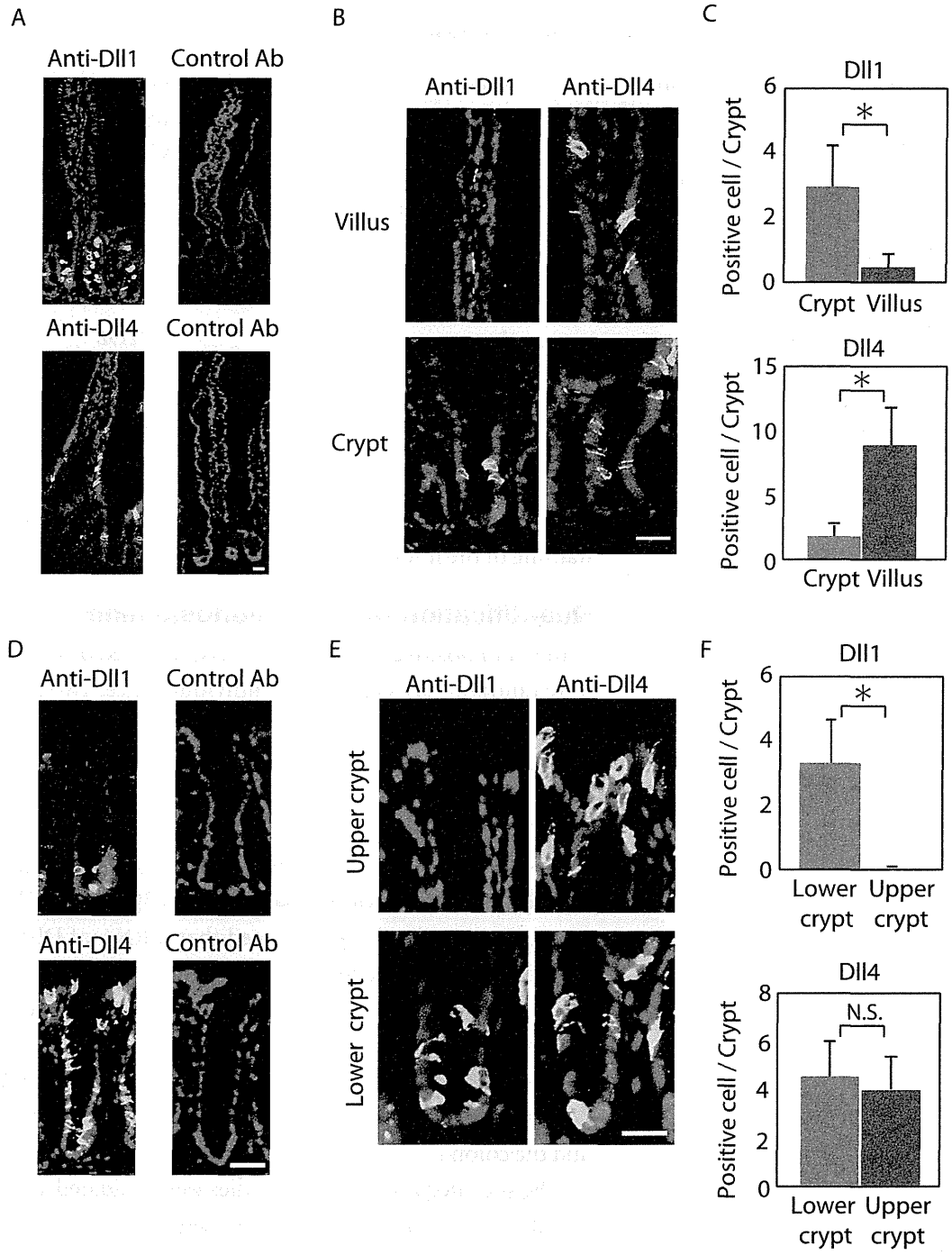

Figure 1 Dll1 and Dll4 are expressed in distinct patterns in the mice gastrointestinal epithelium. Immunohistochemistry of Dll1 and Dll4 were performed using mice small intestinal (A, B) and colonic tissues (D, E). Within the small intestinal epithelium, staining by anti-Dll1 antibody showed positive cells exclusively within the crypt (A, B), whereas staining by anti-Dll4 antibody showed positive cells both in the crypt and in the villi. Quantification of Dll1+ve and Dll4+ve intestinal epithelial cells (IECs) showed that Dll1+ve IECs are predominantly found within the crypt, whereas Dll4+ve IECs are found mostly in the villi (C). In the colonic epithelium, staining by anti-Dll1 antibody showed (continued on next page...)

Figure 1 (...continued)

positive cells exclusively within the lower part of the crypt (D, E), whereas staining by anti-Dll4 antibody showed positive cells both in the lower- and upper part of the crypt, including the surface epithelium. Quantification of Dll1+ve and Dll4+ve IECs showed that Dll1+ve IECs are found exclusively within the lower half of the crypt, whereas Dll4+ve IECs are found both in the lower and upper region of the crypt at a comparable frequency (F). Negative staining of non-immunized isotype antibodies (Control Ab) confirmed the specific staining of Dll1 (A) and Dll4 (D). Scale bar represents 20 μm. Quantitative data are shown as mean ∓ SD of triplicate experiments ($n = 3$). * indicates $P < 0.05$ as determined by Welch's t-test. N.S. indicates not significant.

difference between Dll1-positive (Dll1+ve) and Dll4-positive (Dll4+ve) IECs. In the small intestine, Dll1+ve IECs resided exclusively within the crypts, but were never found in the villi (Fig. 1B). In sharp contrast, Dll4+ve IECs were found both in the villi and in the crypts. Quantitative analysis revealed that Dll1+ve IECs predominantly reside in the crypt, whereas Dll4+ve IECs mostly reside at the villus (Fig. 1C). Such a difference in distribution between Dll1+ve and Dll4+ve IECs were also found in the colon (Figs. 1D and 1E). In the colon, Dll1+ve cells were found predominantly at the lower half of the crypt, but were rarely found at the upper part of the crypt, including the surface epithelium (Fig. 1E). In contrast, Dll4+ve cells were found both in the upper and lower part of the crypt, and also at the surface epithelium. Quantitative analysis confirmed that Dll1+ve IECs reside predominantly in the lower part of the crypt, whereas Dll4+ve IECs reside both in the lower and upper part of the crypt (Fig. 1F). These results indicated that Dll1+ve and Dll4+ve IECs represent a distinct population of cells within the intestinal epithelium.

Both Dll1+ve and Dll4+ve IECs are ATOH1-positive cells, and locate adjacent to Hes1-positive IECs in the small intestinal- and colonic-crypts

Reports have suggested that Hes1 expression in IECs indicate Notch-activation and commitment to absorptive lineage cells, whereas ATOH1 expression in IECs conversely indicates lack of Notch activation and commitment to secretory lineage cells (*van Den Brink, de Santa Barbara & Roberts, 2001*; *Vooijs, Liu & Kopan, 2011*). To identify their potential to serve as Notch activating cells, and gain insight into their cell characteristics, we conducted a double immunostaining analysis of Dll1 or Dll4 with Hes1 or ATOH1. In the small intestinal crypts, both Dll1+ve and Dll4+ve cells were found adjacent to Hes1-positive (Hes1+ve) cells (Figs. 2A and 2B). In the villi, the adjacent cells of Dll4+ve cells were never found to be positive for Hes1. Also, both Dll1+ve and Dll4+ve IECs themselves were never found to be positive for Hes1. Instead, both Dll1+ve and Dll4+ve IECs were invariably positive for ATOH1 (Fig. 2B). Exactly the same expression patterns of Hes1 and ATOH1 within Dll1+ve and Dll4+ve IECs, or in their neighboring cells were found in the colonic crypts (Figs. 2C and 2D). A horizontal cross section of the crypt region further confirmed those expression patterns of Hes1 and ATOH1 in Dll1+ve and Dll4+ve IECs (Fig. S2). These findings clearly illustrate the definite site of lateral inhibition by ATOH1-positive (ATOH1+ve) crypt cells, through their expression of Dll1 or Dll4. In contrast, those Dll4+ve IECs that were found at the small intestinal villi or at the colonic

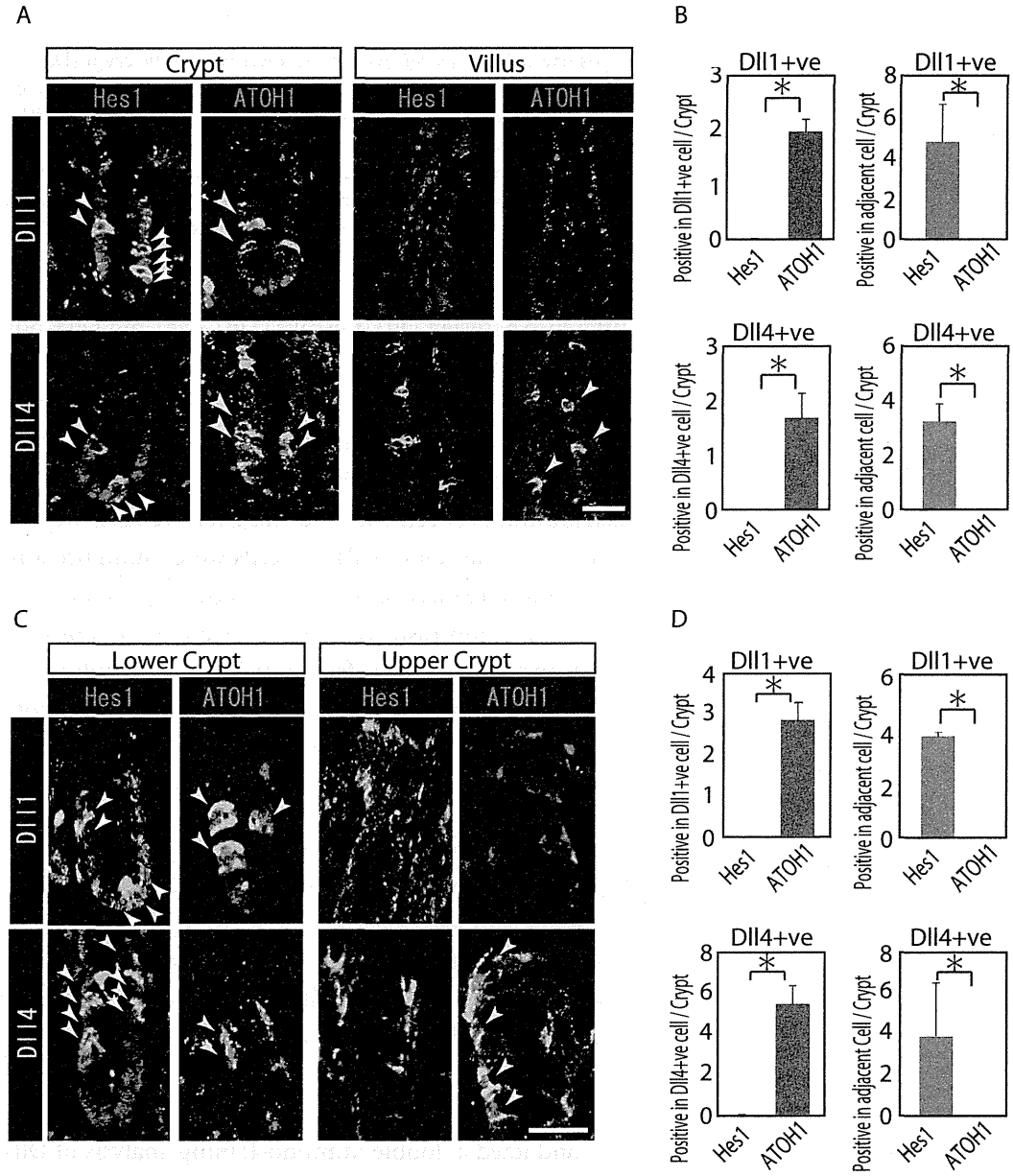

Figure 2 Both Dll1+ve and Dll4+ve IECs are ATOH1+ve IECs, which locate adjacent to Hes1+ve cells within the crypt. (A, C) Double immunostaining of Dll1 or Dll4 (green) with either Hes1 or ATOH1 (red) was performed in the mouse small intestinal (A) and colonic tissues (C). Both in the small intestinal and colonic epithelium, Dll1+ve IECs or Dll4+ve IECs itself were completely negative for Hes1 (yellow arrowhead), but instead, they were found adjacent to Hes1+ve IECs (white arrowhead) within the crypt. Those Dll1+ve IECs or Dll4+ve IECs were invariably positive for ATOH1 (yellow arrowhead). However, those Dll4+ve IECs that were residing at the small intestinal villi or in the colonic surface epithelium were never found adjacent to Hes1+ve IECs. Scale bar represents 20 μm. (B, D) Quantitative analysis of the immunostaining revealed that both Dll1+ve and Dll4+ve IECs are Hes1−ve/ ATOH1+ve cells that locate adjacent to Hes1+ve /ATOH1−ve IECs in the small intestinal (B) and colonic (D) crypts. Quantitative data are shown as mean ∓ SD of triplicate experiments ($n = 3$). * indicates $P < 0.05$ as determined by Welch's t-test. These data were acquired by confocal microscopy (FV10i).

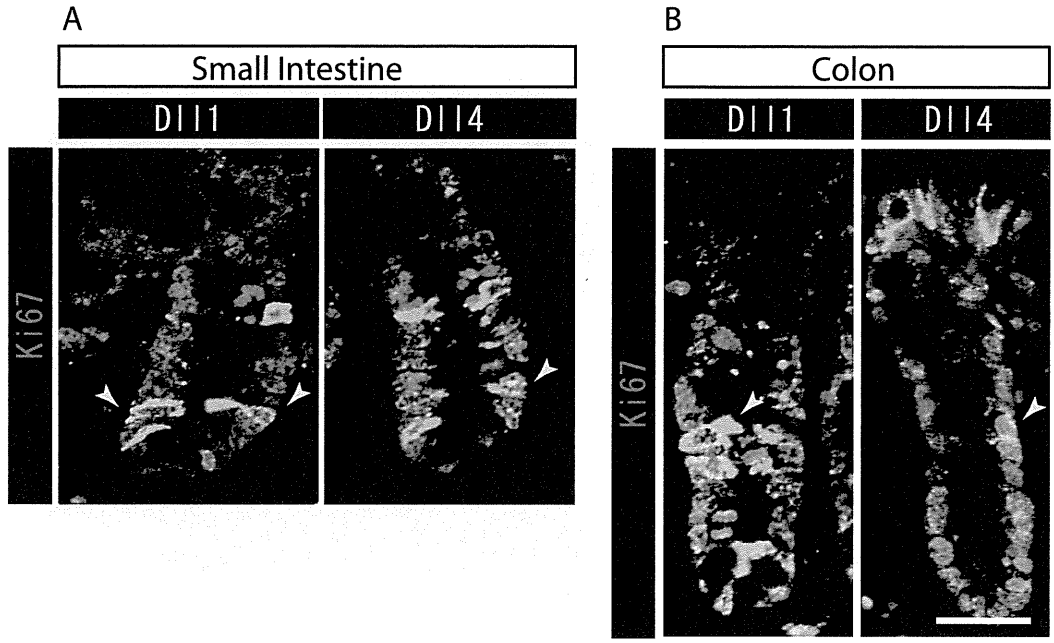

Figure 3 **Both Dll1+ve and Dll4+ve IECs are mostly post-mitotic in the small intestine and in the colon.** Double immunostaining of Dll1 or Dll4 (green) with the proliferation cell marker, Ki67 (red), shows that both Dll1+ve and Dll4+ve IECs are mostly post-mitotic in the small intestine (A) and in the colon (B). However, a small number of Dll1+ve or Dll4+ve IECs that co-express Ki67 can be found (yellow arrowhead). Scale bar represents 20 μm. These data were acquired by confocal microscopy (FV10i).

surface epithelium appeared to co-express ATOH1, but were never found adjacent to Hes1+ve cells, indicating that those IECs may not function as Notch activating cells under normal conditions.

Dll1+ve and Dll4+ve IECs represent distinct populations of secretory lineage cells in the small intestine and in the colon

To further identify the properties of Dll1+ve or Dll4+ve IECs, we further checked the co-expression of a proliferative cell marker, Ki67. Consistent with the former report (*Stamataki et al., 2011*), co-immunostaining with Ki67 showed that both Dll1+ve and Dll4+ve IECs are mostly negative for Ki67, indicating that they are post-mitotic in the small intestine (Fig. 3A) and in the colon (Fig. 3B). Quantitative analysis showed that 34.5% of Dll1+ve IECs and 19.3% of Dll4+ve IECs in the small intestine co-express Ki-67 (Table S1). Also, 22.6% of Dll1+ve IECs and 14.8% of Dll4+ve IECs in the colon co-expressed Ki-67. However, those values varied among individual crypts. As our former results suggested that both Dll1+ve and Dll4+ve IECs are ATOH1+ve cells that are committed to the secretory cell lineage, we analyzed the expression of secretory lineage differentiation markers in Dll1+ve or Dll4+ve IECs. In the small intestine, both Dll1+ve and Dll4+ve goblet cells were clearly present (Fig. 4A). Also, a few number of Dll4+ve enteroendocrine cells were found (Table S1). However, enteroendocrine cells that are positive for Dll1, or tuft cells that are positive for either Dll1 or Dll4, were never observed.

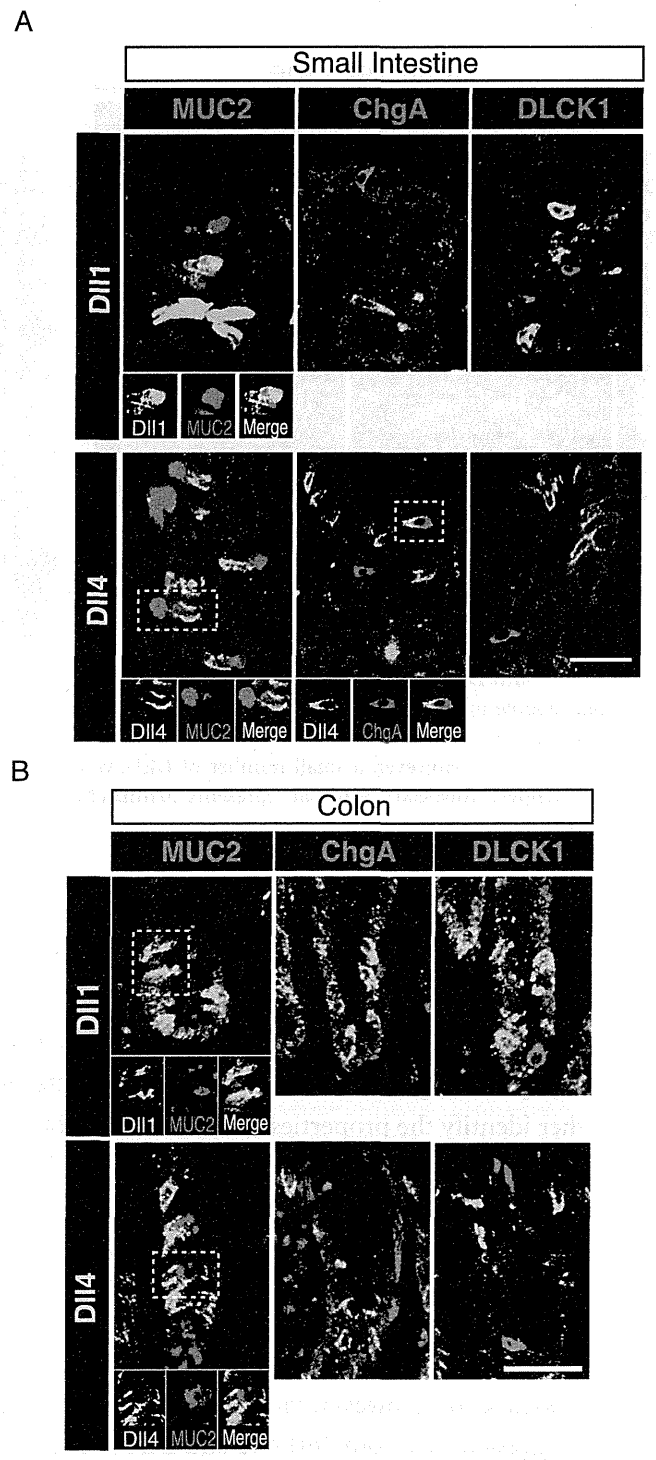

Figure 4 **Dll1+ve and Dll4+ve IECs represent distinct populations of secretory lineage cells in the small intestine and in the colon.** Double immunostaining of Dll1 or Dll4 with various secretory cell lineage markers were performed. (A) Immunostaining of Dll1 or Dll4 (green) with Muc2 (goblet cells, red), ChgA (Enteroendocrine cells, red) or DLCK1 (Tuft cells, red) using the small intestinal tissues shows that both Dll1+ve and Dll4+ve cells can co-express Muc2 (white square). (continued on next page...)

Figure 4 (...continued)

Also, a small number of Dll4+ve cells that co-express ChgA were present (white square). However, Dll1+ve IECs were never found positive for ChgA or DLCK1. Also, Dll4+ve IECs were never found positive for DLCK1. Scale bar represents 20 μm. A magnified view of the area marked with a white square is shown in the lower panel. (B) The same immunostaining shown in (A) was performed using the colonic tissues. Both Dll1+ve and Dll4+ve colonic IECs can also co-express Muc2 (white square). However, both Dll1+ve and Dll4+ve IECs were never found positive for ChgA or DLCK1. Scale bar represents 20 μm. A magnified view of the area marked with a white square is shown in the lower panel. These data were acquired by confocal microscopy (FV10i).

In the colon, both Dll1+ve and Dll4+ve goblet cells were also clearly present (Fig. 4B). However, enteroendocrine cells or tuft cells that are positive for Dll1 or Dll4 were never observed. Quantitative analysis showed that increased number of Dll4+ve IECs co-express MUC2, compared to Dll1+ve IECs, both in the small intestine and in the colon (Table S1). Thus, the results indicated that both Dll1+ve and Dll4+ve IECs could acquire goblet cell phenotype, but rarely exhibit the phenotype of other secretory lineage cells. However, as compared to Dll1+ve IECs, Dll4+ve IECs appeared to include higher number of terminally differentiated goblet cells and can additionally acquire enteroendocrine cell phenotype, which confirmed the idea that Dll1+ve and Dll4+ve IECs represent distinct population of secretory lineage cells.

Dll1+ve or Dll4+ve IECs constitute the intestinal stem cell niche

Previous studies have suggested that Paneth cells express Dll1 or Dll4, and thereby constitute the key component of the small intestinal stem cell niche (*Stamataki et al., 2011*; *Sato et al., 2012*). However, endogenous protein expression of Dll1 or Dll4 in those stem cell niche cells has never been demonstrated. So far, our immunohistochemical analysis of small intestinal tissues failed to detect expression of Dll1 in any Paneth cell (Fig. 5A). However, a clear expression of Dll4 was found in a very rare population of Paneth cells (Fig. 5B). In the colon, it has been shown that c-kit positive cells take the place of Paneth cells, and constitute the colonic stem cell niche (*Rothenberg et al., 2012*). Double immunostaining with c-kit clearly showed that Dll1+ve IECs mostly overlap with the c-kit-positive cell population in the colon (Fig. 5C). Also, those Dll4+ve IECs that reside at the lower part of the colonic crypts clearly co-expressed c-kit (Fig. 5D). Quantitative analysis showed that almost all Dll1+ve IECs are c-kit positive, whereas around 70% of Dll4+ve IECs are c-kit positive in the colon (Table S1). Thus, our analysis showed that Dll1+ve IECs or Dll4+ve IECs surely reside as a component of the stem cell niche in small intestinal and colonic crypts.

On the other hand, our analysis of Lgr5-EGFP-ires-CreERT2 mice showed that Dll1+ve IECs or Dll4+ve IECs are mostly negative for LGR5-EGFP, suggesting that those cell populations do not include the LGR5-positive stem cell itself. However, we found a rare population of Dll1+ve or Dll4+ve IECs that co-express LGR5-EGFP, at the upper end of the stem cell region (Fig. S3). Those cells appeared to express EGFP at a relatively low level, and preferentially located at the +5 position. Thus these Dll1+EGFP+double

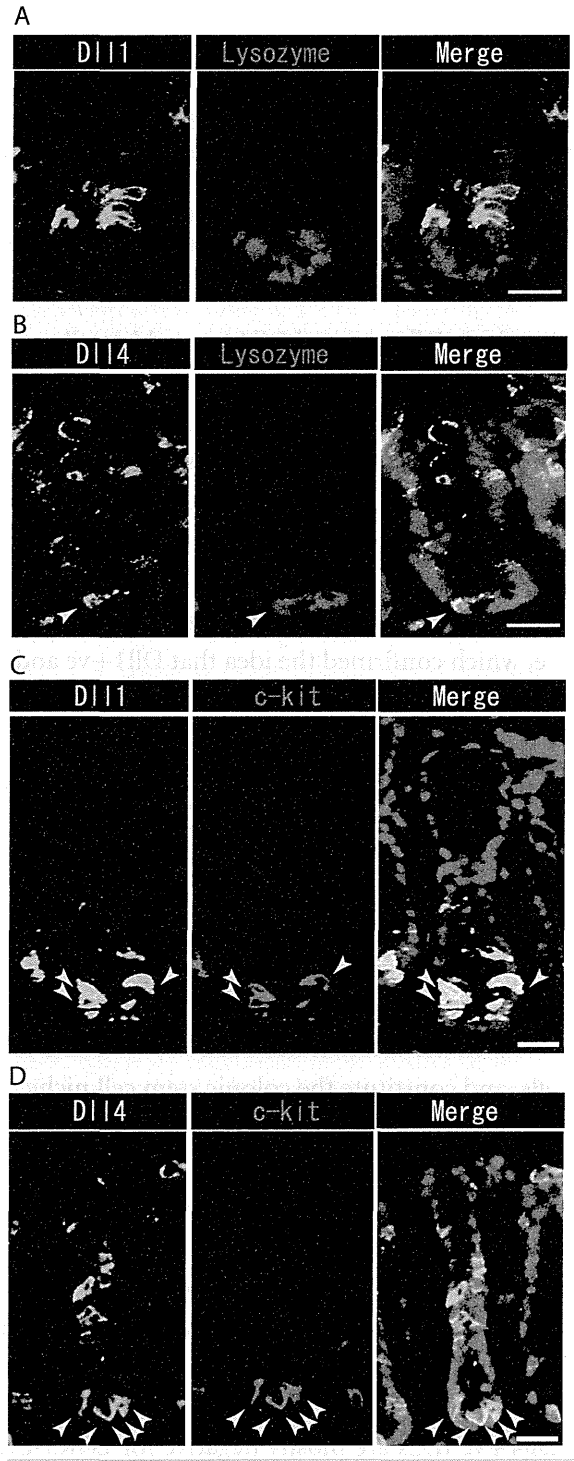

Figure 5 Dll1+ve or Dll4+ve IECs constitute the intestinal stem cell niche. Double immunostaining of Dll1 or Dll4 with a stem-cell niche cell marker, Lysozyme or c-kit, was performed in the mice small intestine and in the colon, respectively. (A) Immunostaining of Dll4 (green) with Lysozyme (red) shows that Dll4 is expressed in Paneth cells of the small intestine (yellow arrowhead). Scale bar represents 20 μm. (B) Double immunostaining of Dll1 (green) and c-kit (red) shows that (continued on next page...)

Figure 5 (...continued)

Dll1+ve colonic IECs mostly co-express c-kit (yellow arrowhead). Also, double immunostaining of Dll4 (green) and c-kit (red) showed that a distinct population of Dll4+ve cells co-express c-kit (yellow arrowhead). Scale bar represents 20 μm.

positive cells, or Dll4+EGFP+double positive cells may represent the bi-potent secretory progenitor cells as described previously by *van Es et al. (2012)*.

Dll4+ve cells dominate the colonic crypts of the DSS-colitis mice

Our previous study has shown that number of Hes1+ve cells significantly increase in the colitic mucosa of DSS-colitis mice, and also in ulcerative colitis patients, indicating that the canonical Notch pathway is activated in those cells (*Okamoto et al., 2009*; *Zheng et al., 2011*). However, the ligand that is responsible for such an increase in Notch activation remains uncertain. Therefore, we examined the expression of Dll1 and Dll4 in tissues of DSS-colitis mice. Analysis showed a surprising loss of Dll1 expression in the crypts of DSS-colitis mice (Fig. 6A). Conversely, a striking increase in the number of Dll4+ve IECs was observed in the crypts of those DSS-colitis mice, suggesting that a distinct regulation of Dll1 and Dll4 expression exists under the inflammatory environment. Quantitative analysis confirmed that number of Dll1+ve IECs significantly decrease, whereas that of Dll4+ve IECs significantly increase in DSS-colitis mice, compared to control mice (Fig. 6B). Double staining with Hes1 confirmed that a rare population of Dll1+ve IECs, as well as the dominant Dll4+ve IECs clearly located adjacent to Hes1+ve IECs within the elongated crypts of the DSS-colitis mice (Fig. 6C). Of note, those Hes1+ve IECs appearing at the mid-to-upper part of the colitic crypts were mostly accompanied adjacently by Dll4+ve IECs. Also, the analysis showed that both Dll1+ve and Dll4+ve IECs that were found in the DSS-colitis mice maintain their expression of ATOH1 (Fig. 6D). A horizontal cross section of the lower and upper crypt region further confirmed those expression patterns of Hes1 and ATOH1 in Dll4+ve IECs (Fig. S4). Thus, results indicated that the Dll1- or Dll4-ligand mediated Notch activation, as well as the lateral inhibition system, is maintained and present also in the inflamed colonic crypts.

DISCUSSION

In the present study, we showed that Dll1 and Dll4 are expressed in distinct patterns along the crypt-villus axis of the small intestine and the colon. The present distribution of Dll1 and Dll4 raised a possibility that ATOH1+ve secretory progenitor cells might express Dll1 at their earlier stage, and subsequently develop into Dll4+ve IECs as they become fully differentiated into goblet cells or enteroendocrine cells. Such a sequential expression of Dll1 and Dll4 during the process of lineage commitment has been formerly reported in the retina (*Rocha et al., 2009*). Former analysis by Stamataki et al., using Dll1-LacZ reporter mice, showed that Dll1+ve IECs overlap with Dll4+ve IECs in the mice small intestine (*Schröder & Gossler, 2002*). Such a complete overlap may due to the relatively longer half-life of the LacZ protein, compared to the endogenous Dll1 protein, and further

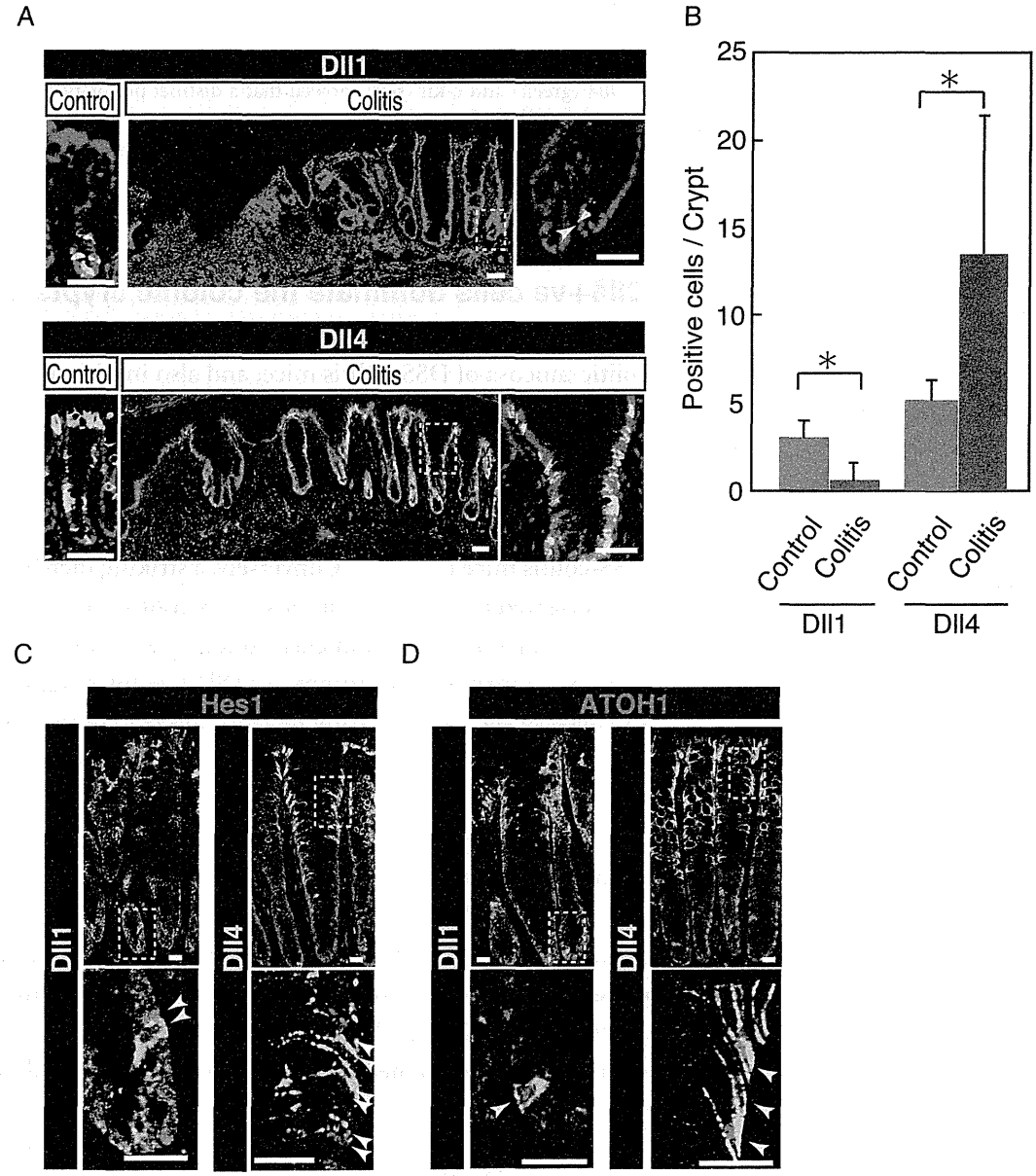

Figure 6 **Dll4+ve cells dominate the colonic crypts of the DSS-colitis mice.** Immunohistochemical analysis of colonic tissues that were prepared from DSS-colitis mice is shown. (A) Immunostaining of Dll1 and Dll4 using the inflamed colonic tissue of the DSS-colitis mice at day 10 (Colitis), or the corresponding tissue of the control mice (Control). In the inflamed colon, Dll1+ve IECs (green, upper panel) were rarely found within the crypts (yellow arrowhead). In sharp contrast, Dll4+ve IECs were frequently found, which dominated the entire crypt and also the surface epithelium. A magnified view of the area marked with a white square is shown in the right-end panel. Scale bar represents 50 μm. (B) Quantitative analysis of the staining shown in (A). Data shows a significant decrease in number of Dll1+ve IECs in the DSS-colitis mice ($n = 3$), compared to the control mice ($n = 3$). In contrast, a significant increase was found in number of Dll4+ve IECs in the DSS colitis mice, compared to control mice. Quantitative data are shown as mean ∓ SD. * indicates $P < 0.05$ as determined by Welch's t-test. (C) Double immunostaining of Hes1 (red) with either Dll1 or Dll4 (green). In the DSS-colitis mice, Hes1+ve cells were increased in number, and distributed up to the upper (continued on next page...)